Climate-Adaptive Materials Engineering

Journal Homepage: https://journals.explorerpress.com/came

Research Article

Investigation of Thermal Stress Performance of Si_3N_4 Discs for Aerospace Applications

Hüseyin Fırat KAYIRAN

Agricultural and Rural Development Support Institution, Mersin, Turkey

KEYWORDS

thermoelasticity
aerospace
applications
silicon nitride (Si_3N_4)

ABSTRACT

The behavior of a disk made of silicon nitride (Si_3N_4) under thermal loads was investigated using numerical analysis. Due to its superior properties such as high thermal resistance, low coefficient of thermal expansion, and high fracture toughness, Si_3N_4 stands out among advanced ceramic materials. Owing to these characteristics, it is widely used in gas turbine engine components, bearing systems, cutting tools, and engineering elements operating at high temperatures. In this study, it was assumed that the elastic modulus does not vary with temperature, and a formulation describing this relationship was derived. Thermal analyses were conducted at temperature levels of 80 °C, 100 °C, 120 °C, 140 °C, and 160 °C. The results revealed that with increasing temperature, both radial and tangential stresses rise in magnitude. Furthermore, it was determined that tangential stresses are significantly higher compared to radial stresses.

*CORRESPONDING AUTHOR

Hüseyin Fırat KAYIRAN, Agricultural and Rural Development Support Institution, Mersin, Turkey; Email: huseyinfiratkayiran@gmail.com

ARTICLE INFO

Received: 1 September 2025 | Revised: 27 September 2025 | Accepted: 28 September 2025 | Published Online: 29 September 2025
DOI: https://doi.org/10.65773/came.1.1.24

1. Introduction

Functionally graded materials (FGMs) have attracted considerable attention in recent years for use in rotating disks and cylindrical structures due to their superior mechanical and thermal performance under demanding operating conditions such as high temperatures and high rotational speeds. In particular, the investigation of the elastic, thermoelastic, and elastoplastic behavior of disks with variable thickness, multilayered configurations, or coatings is of critical importance for aerospace, energy, and defense applications. Various methods and approaches have been developed in the literature on this subject. For example, Eldeeb, Shabana, and Elsawaf [1] investigated the effects of angular deceleration on the thermoelastoplastic behavior of multilayered FGMs with nonuniform thickness, highlighting the complex stress distributions in such disks. Similarly, Afsar, Go, and Song [2] analytically modeled the thermoelastic properties of rotating disks with an FGM coating on the outer surface, demonstrating the critical role of the coating. The direct integration method developed by Tokovyy and Ma [3] has provided an important theoretical basis for the elastic analysis of heterogeneous solids. Yıldırım [4] contributed to the field by addressing the elastic behavior of arbitrarily graded polar orthotropic rotating disks through both numerical and analytical solutions. Furthermore, Zhao, Dang, Fan, and Chen [5] presented theoretical solutions for analyzing arbitrarily shaped interfacial cracks in three-dimensional isotropic thermoelastic bimaterials. More recently, Dai et al [6]. examined the thermo-mechanical behavior of multilayered cylindrical thermal protection structures with ultra-high temperature ceramic layers, while Iqbal et al [7]. analyzed thermoelastic fracture problems in FGMs using the scaled boundary finite element method. This body of literature demonstrates that FGMs are critical to ensuring both structural integrity and thermal resistance, and they must be extensively evaluated in modern engineering applications. In this study, it is assumed that the elastic modulus of the material does not vary with temperature, and thermal stress analysis is performed for each temperature condition. Silicon nitride (Si_3N_4) stands out among advanced ceramic materials due to its superior properties such as high fracture toughness, excellent wear resistance, low thermal expansion coefficient, and outstanding thermal shock resistance [8]. This combination of properties makes Si_3N_4 an ideal candidate for the most demanding engineering challenges in the aerospace sector. Indeed, it has been widely employed in critical applications such as high-speed rotating bearings, gas turbine blades, and structural components exposed to sudden temperature fluctuations [9]. However, in such applications, the long-term reliability and service life of the material are directly related to its performance under thermal loads and the resulting thermal stresses. Despite its low coefficient of thermal expansion, the internal constraints generated under high thermal gradients can lead to thermal stresses that may exceed the fracture toughness of the material [10]. Therefore, accurate thermal stress analysis during the design stage of components is of great importance. Within the scope of this study, the thermal stress behavior of Si_3N_4 disk geometries is examined using an integrated approach combining experimental and numerical methods. In this way, the study aims to provide fundamental data for the prediction of material service life and the establishment of safe design criteria. Critical stress regions determined by finite element analysis (FEA) will be validated with experimental stress measurements, thereby clarifying the thermomechanical limits of the material.

2. Material and Method

In this numerical study, the thermal stress behavior of the silicon nitride (Si_3N_4) disk was investigated under thermal loading corresponding to temperature differences of 80 °C, 100 °C, 120 °C, 140 °C, and 160

°C (Figure 1). The analyses were carried out based on the assumption that the disk thickness is small compared to its diameter. Under this assumption, the disk thickness was taken as unity, and for the plane stress condition,σz = 0 was assumed. For a thin disk, the general equilibrium equation in the radial direction, as given by Timoshenko and Goodier [11], is expressed as follows:"

$$\frac{r(d\sigma_r)}{dr} + (\sigma_r) - (\sigma_\theta) = 0 \tag{1}$$

It is expressed as follows. In Equation (1), r denotes the radius of the disk at any point, σ_r represents the radial stress, and σ_θ denotes the tangential stress. Here, the disk material is taken as $i = 1$.

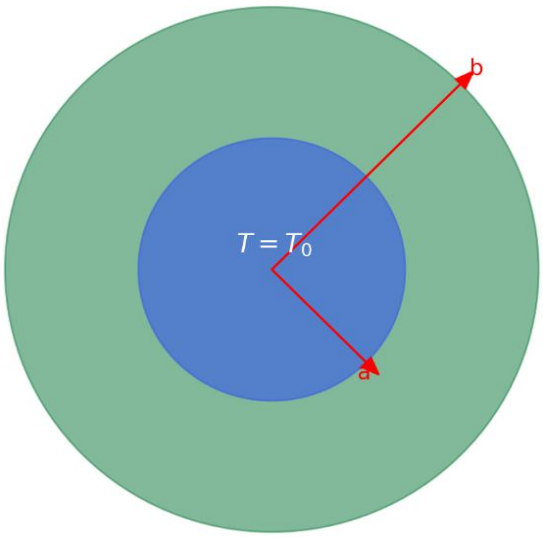

Figure 1. A disk subjected to thermal stress analysis.

$$\varepsilon_r = \frac{du}{dr} \tag{2}$$

$$\varepsilon_\theta = \frac{u}{r} \tag{3}$$

Here, **u** denotes the radial displacement, $\boldsymbol{\varepsilon_r}$ represents the radial strain, and $\boldsymbol{\varepsilon_\theta}$ denotes the tangential strain. The strain–stress relationship [11] is expressed as follows:

$$\varepsilon_{ri} = \frac{1}{E}(\sigma - \upsilon\sigma_\theta) + \alpha T \tag{4}$$

$$\varepsilon_\theta = \frac{1}{E}(\sigma_\theta - \upsilon\sigma_r) + \alpha T \tag{5}$$

$$\sigma_r = \frac{F}{r} \tag{6}$$

$$\sigma_\theta = \frac{dF}{dr} \tag{7}$$

It is expressed as follows. When equations (6) and (7) are substituted into equations (4) and (5);

$$\varepsilon_r = \frac{1}{E}\left(\frac{F}{r} - \upsilon\frac{dF}{dr}\right) + \alpha T_r \tag{8}$$

$$\varepsilon_\theta = \frac{1}{E}\left(\frac{dF}{dr} - \upsilon\frac{F}{r}\right) + \alpha T_r \tag{9}$$

$$\frac{d\,\varepsilon_\theta}{dr} + \varepsilon_\theta - \varepsilon_r = 0 \tag{10}$$

$$r^2\frac{d^2F}{dr^2} + r\frac{dF}{dr} - F = -\,r^2\alpha E T_r^{'} \tag{11}$$

It is thus obtained. By employing the equilibrium equation, in which the stress function is defined as *F*, together with Equations (1)–(7), the general Equation (11) is derived.

$$\sigma_r = C_1 + C_2 r^{-2} + Ar^2 \tag{12}$$

$$\sigma_\theta = C_1 - C_2 r^{-2} + 3Ar^2 \tag{13}$$

Using the boundary conditions r=a and r=b where σr=0, the integration constants C1, C2 the final term A_i are determined as follows:

$$A_i = \frac{E\alpha T_0}{4(b^2 - a^2)} \tag{14}$$

$$C_1 = -\,A(a^2 + b^2) \tag{15}$$

$$C_2 = A(a^2 b^2) \tag{16}$$

The radial displacement uuu is obtained as given in equation (17);

$$(U_r)_i = \left[\frac{1}{E_i}\left(C_1 r(1 - \upsilon_i) - \frac{C_2}{r}(1 - \upsilon_i) + A_i\, r^3(3 - \upsilon_i)\right) + \alpha_i r T\right]_i \tag{17}$$

3. Results and Discussion

In this study, the thermal stresses induced in a silicon nitride (Si_3N_4) disk element subjected to constant temperature differences applied from the inner surface to the outer surface were investigated. The disk was structurally constrained, with an inner radius (*a*) of 45 mm and an outer radius (*b*) of 90 mm, as illustrated in Figure 1. Analyses were carried out for temperature differences of 80 °C, 100 °C, 120 °C, 140 °C, and 160 °C, and the corresponding stress distributions under these thermal loadings were computed. The solutions were obtained under two different assumptions: (i) the elastic modulus (*E*) remains constant with temperature,

and (i) the elastic modulus varies with temperature. The calculated radial (σ_r) and circumferential (σ_θ) stress values for both cases are presented comparatively in the form of graphs and tables. The thermophysical properties of the silicon nitride material used are given in Table 1.

Silicon nitride (Si_3N_4) ceramics are widely employed in advanced engineering applications due to their high hardness, low density, and excellent resistance to thermal shock [12]. This material maintains its mechanical strength at elevated temperatures, exhibits outstanding wear and corrosion resistance, and provides long-term performance owing to its low coefficient of friction, making it particularly suitable for industrial and structural ceramic applications [13]. Furthermore, with a density of approximately 3.2 g/cm³ and an elastic modulus around 300 GPa, Si_3N_4 demonstrates low thermal expansion and high compressive strength, which render it highly reliable in environments requiring durability under high speed and high temperature conditions [14].

Table 1. Material properties of Silicon Nitride (Si_3N_4) [12-14].

Property	Symbol	Value	Unit
Elastic Modulus	E	310	GPa
Poisson's Ratio	ν	0.28	-
Coefficient of Thermal Expansion	α	3.2 x 10^{-6}	1/°C
Density	ρ	3200	kg/m³

The mathematical results obtained from the analysis are presented in Table 2 below.

Table 2. Tangential stress σt and radial stress σrvalues at the inner and outer surfaces of the silicon nitride (Si_3N_4) disk

Temperature ΔT (°C)	Surface	Stresses		Displacement
		σt (MPa)	σr (MPa)	Ur (mm)
80	Inner (r=45)	-14.063	0	0.0103
	Outer (r=90)	33.563	0	0.3211
100	Inner (r=45)	-28.125	0	0.0118
	Outer (r=90)	67.127	0	0.3862
120	Inner (r=45)	-42.188	0	0.0148
	Outer (r=90)	100.690	0	0.4499
140	Inner (r=45)	-56.507	0	0.0162
	Outer (r=90)	134.254	0	0.5150
160	Inner (r=45)	-70.313	0	0.0192
	Outer (r=90)	167.817	0	0.5786
180	Inner (r=45)	-87.188	0	0.0207
	Outer (r=90)	208.093	0	0.6438

Figure 2. Comparative distribution of radial stresses (σ_r) at the inner and outer surfaces of the silicon nitride (Si_3N_4) disk under different thermal loadings

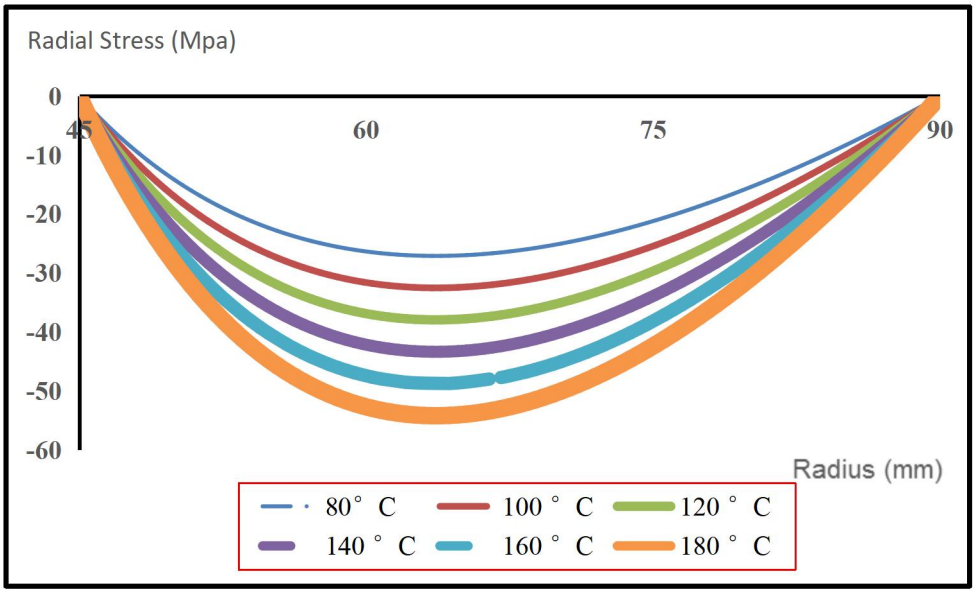

Figure 2. Variation of radial stresses (σ_r) observed at the inner and outer surfaces of the silicon nitride (Si_3N_4) disk as a function of the applied temperature difference (ΔT)

According to the computational results for the Si_3N_4 disk presented in Figure 2: at 100 °C, the radial stress at a point close to the inner region of the disk ($r \approx 46.5$ mm) is approximately −6.05 MPa based on linear interpolation; at 180 °C, the stress at the same location is approximately −10.08 MPa. The radial stresses are compressive in nature at all temperatures. Their magnitude increases radially from the inner to the outer surface, reaching a peak around $r \approx 63.5$ mm (e.g., ≈ −54.23 MPa at 180 °C), and then gradually decreases. Therefore, for the Si_3N_4 disk, the maximum compressive stress does not occur very close to the inner surface but rather in the mid-radius region ($r \approx 63$–64 mm).

Figure 3. Comparative distribution of tangential stresses (σ_t) at the inner and outer surfaces of the silicon nitride (Si_3N_4) disk under different thermal loadings

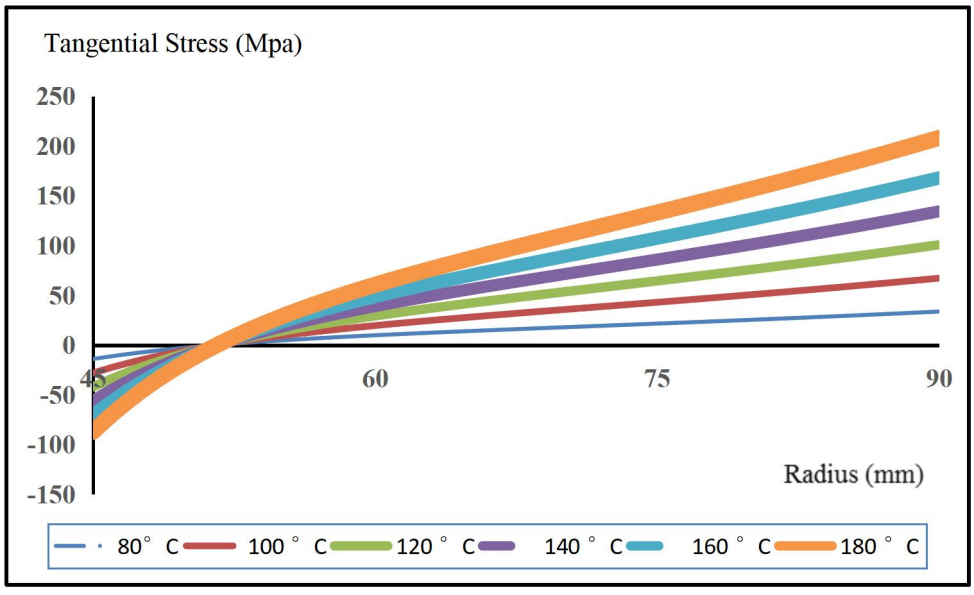

Figure 3. Variation of tangential stresses (σ_t) observed at the inner and outer surfaces of the silicon nitride (Si_3N_4) disk as a function of the applied temperature difference (ΔT).

According to the results presented in Figure 3, when the tangential stresses of the Si_3N_4 disk are examined, at 100 °C the stress at the inner edge (r = 45 mm) is −28.13 MPa, showing a compressive nature. As the radius increases, this value gradually decreases; for instance, at r = 49.5 mm the tangential stress decreases to −7.06 MPa. Toward the outer edge, the stresses change sign, becoming tensile in nature and increasing significantly. At the same temperature, the tangential stress at the outer edge (r = 90 mm) reaches +67.13 MPa. A similar trend is maintained at higher temperatures; compressive stresses at the inner edge grow in magnitude, while tensile stresses at the outer edge also increase. For example, at 180 °C the tangential stress at the inner edge (r = 45 mm) is −87.19 MPa, at the mid-region (r = 49.5 mm) it is −21.88 MPa, and at the outer edge (r = 90 mm) it reaches +208.09 MPa. Thus, for the Si_3N_4 disk, tangential stresses transition from compression to tension moving outward from the inner to the outer surface, and these values increase significantly with temperature.

Figure 4. Comparative distribution of radial displacements (U_r) at the inner and outer surfaces of the silicon nitride (Si_3N_4) disk under different thermal loadings

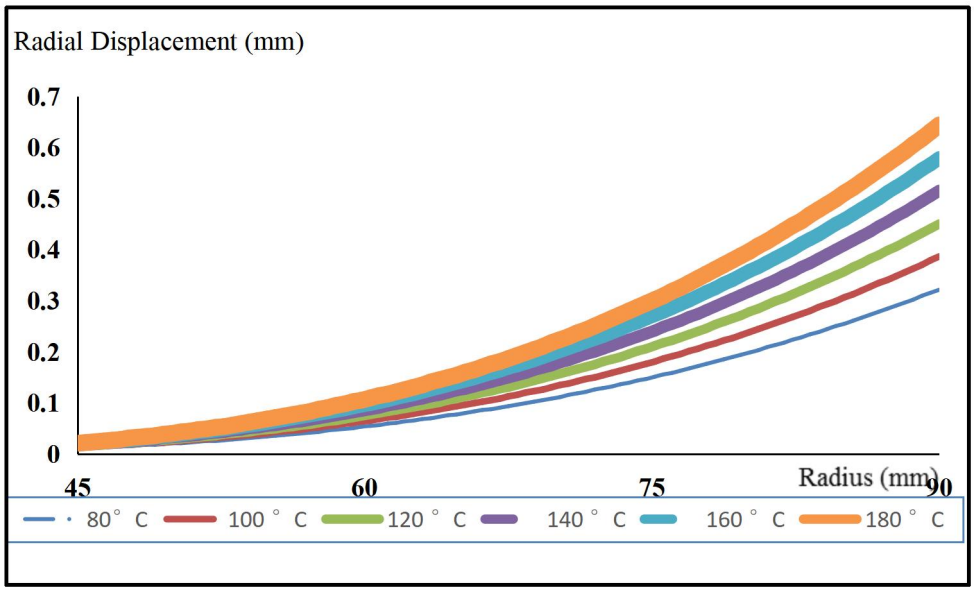

Figure 4. Variation of radial displacements (U_r) observed at the inner and outer surfaces of the silicon nitride (Si_3N_4) disk as a function of the applied temperature difference (ΔT).

According to the tables presented in Figure 5, for the Si_3N_4 disk, the radial displacement (u_r) increases systematically with both radius and temperature. At 100 °C, the displacement at the inner edge (r = 45 mm) is approximately 0.01184 mm, increasing to about 0.07 mm in the mid-region (r ≈ 60 mm), and reaching about 0.386 mm at the outer edge (r = 90 mm). At 160 °C, the corresponding displacements are ≈ 0.019 mm, ≈ 0.10 –0.11 mm, and ≈ 0.579 mm, respectively; while at 180 °C, they reach ≈ 0.0207 mm → 0.11–0.12 mm → 0.644 mm. The curve shapes are convex at all temperatures; the rate of increase grows with radius, and the maximum displacement always occurs at the outer edge. These results indicate that thermal expansion and temperature rise cause a monotonic radial enlargement of the disk, with displacement increasing markedly from the inner to the outer region.

Figure 5. Tangential stresses occurring at the inner and outer regions of the silicon nitride (Si_3N_4) disk.

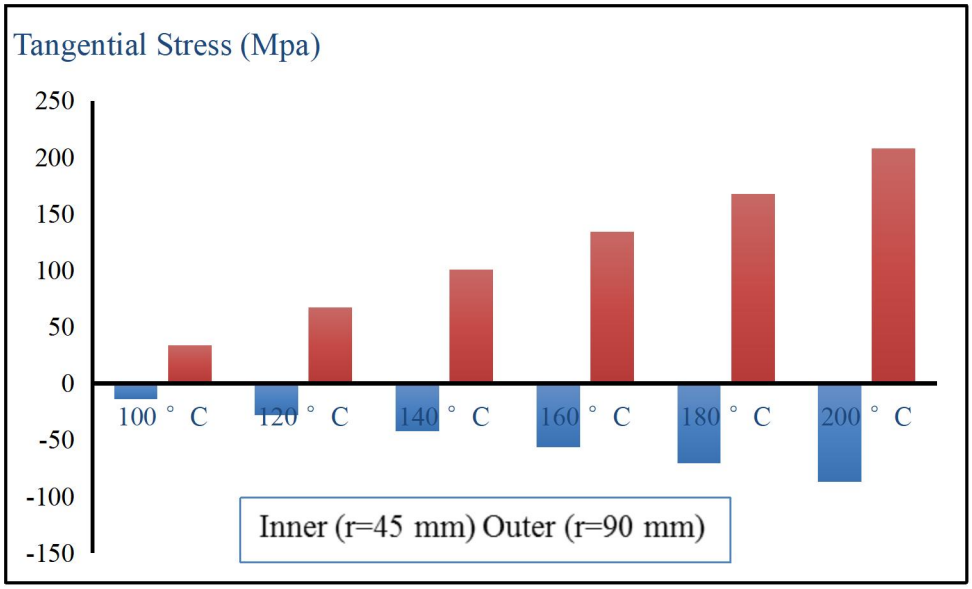

Figure 5. Representation of tangential stresses occurring at the innermost and outermost regions of the disk

The results obtained are visually presented below in Figure 6 for 100 °C.

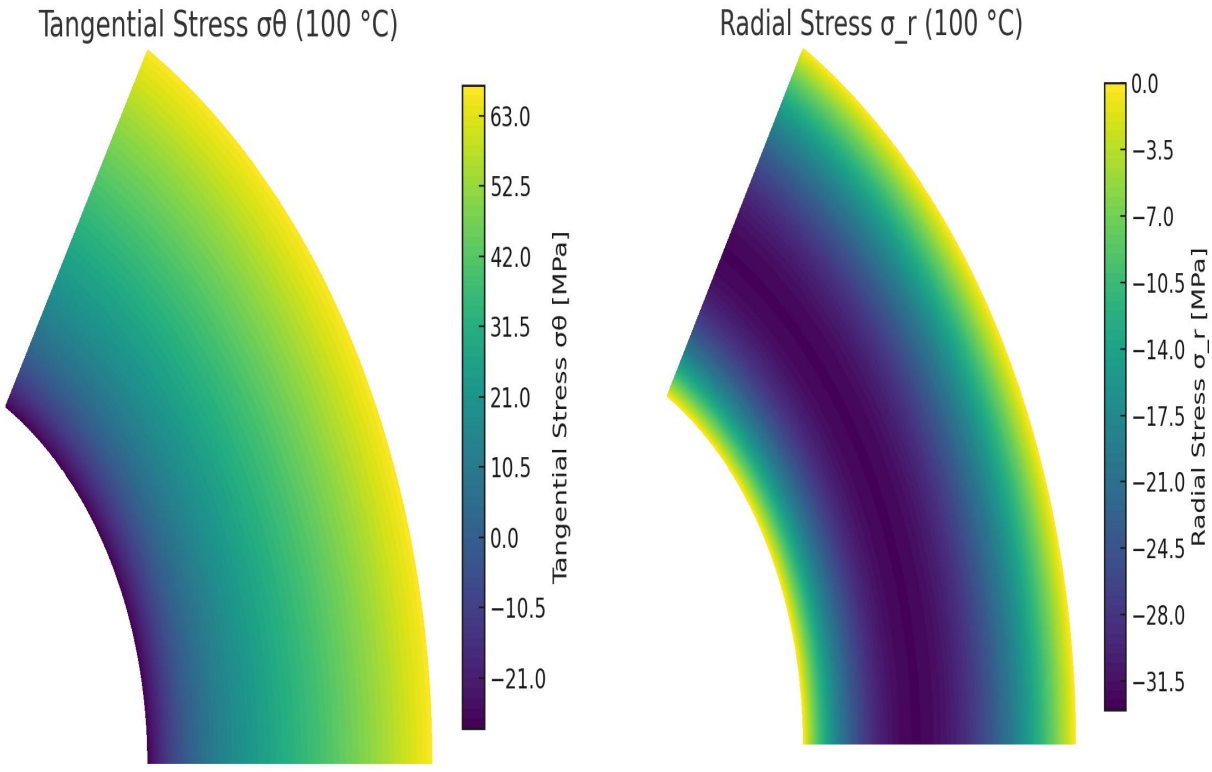

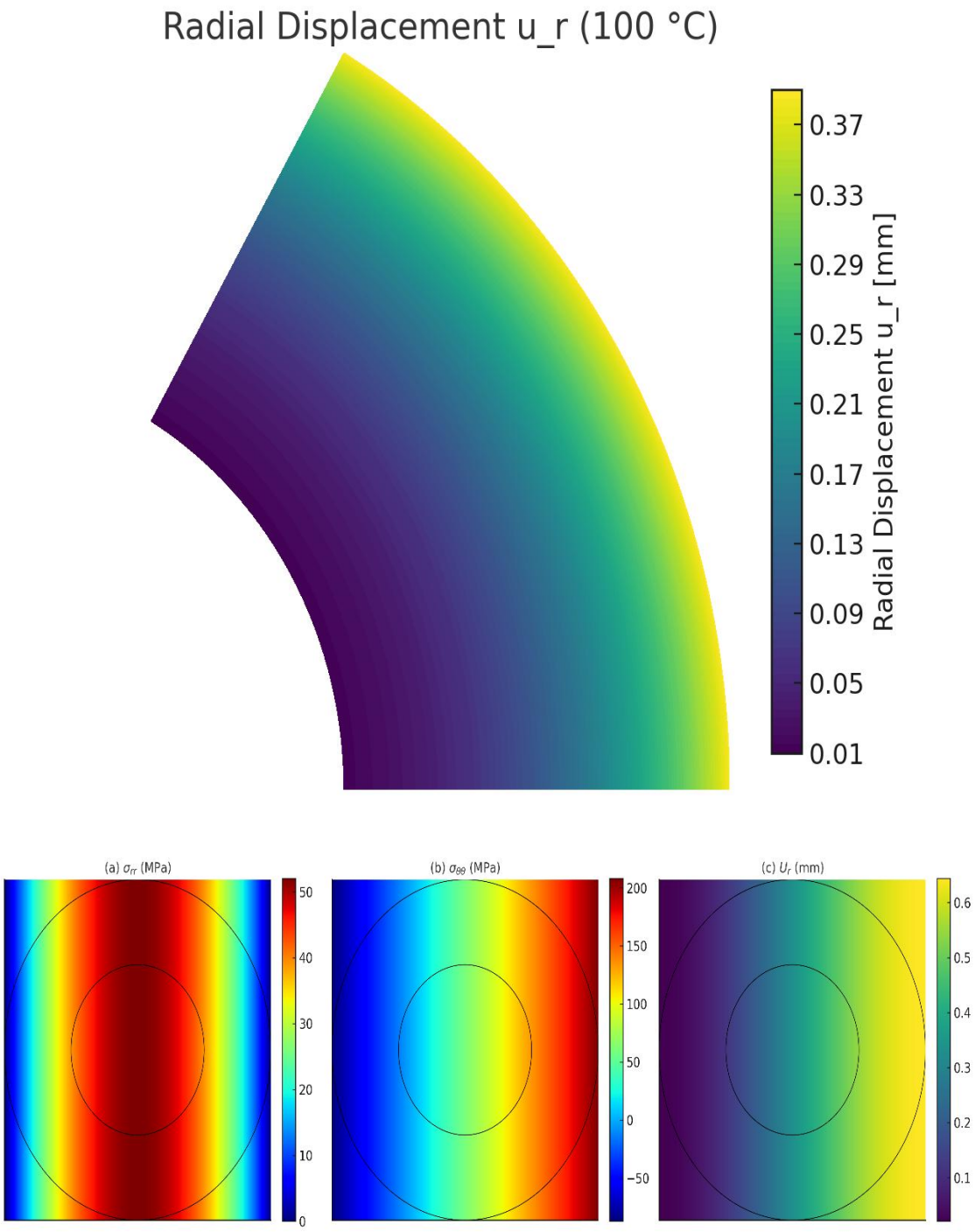

Figure 6. Visual representation of the results for the Si_3N_4 disk at 100 °C.

4. Conclusion

In this study, the thermal stress performance of Si_3N_4 disks intended for aerospace applications was investigated. The distributions of radial and tangential stresses occurring across the disk, from the inner to the outer surface, were analyzed in detail. The analyses confirmed that the radial stress components in the disk are always zero at both the inner and outer surfaces. According to the tabulated results, both tangential stress (σ_t) values and radial displacement (U_r) values increase with rising temperature.

- At the inner surface (r = 45 mm), tangential stress was compressive (negative) at all temperatures, and its magnitude increased as the temperature rose. For example, at 100 °C the tangential stress was −14.06 MPa, while at 200 °C it reached −87.19 MPa.
- At the outer surface (r = 90 mm), tangential stress was tensile (positive) at all temperatures. The value increased from 33.56 MPa at 100 °C to 208.09 MPa at 200 °C.
- Radial displacement (Ur) values also rose significantly with temperature. At the inner surface, the displacement increased from 0.01036 mm at 100 °C to 0.02072 mm at 200 °C, while at the outer surface it grew from 0.32116 mm to 0.64380 mm.

These findings demonstrate that both compressive and tensile stresses grow markedly with increasing temperature. In particular, at elevated temperatures, Si_3N_4 (silicon nitride) disks exhibit higher strength compared to conventional materials such as cast iron, aluminum, and bronze. This highlights Si_3N_4 disks as promising candidate materials for aerospace and aviation industries, where high temperature resistance and mechanical strength are critical requirements.

Funding

This research did not receive any external funding.

Data Availability

The data supporting the findings of this published article are available from the author [HFK] upon request.

Conflict of Interest

The authors declare that there are no conflicts of interest.

Acknowledgments

I would like to express my deepest gratitude to my family for their unwavering support throughout this article.

References

[1] Eldeeb, A. M., Shabana, Y. M., & Elsawaf, A. (2021). Influences of angular deceleration on the thermoelastoplastic behaviors of nonuniform thickness multilayer FGM discs. Composite Structures, 258, 113092. https://doi.org/10.1163/092430410X490482

[2] Afsar, A. M., Go, J., & Song, J. I. (2010). A mathematical analysis of thermoelastic characteristics of a rotating circular disk with an FGM coating at the outer surface. Advanced Composite Materials, 19(3), 269–288. https://doi.org/10.1016/j.compstruct.2020.113092

[3] Tokovyy, Y., & Ma, C.-C. (2021). The direct integration method for elastic analysis of nonhomogeneous solids. Cambridge Scholars Publishing.

[4] Yıldırım, V. (2018). Numerical/analytical solutions to the elastic response of arbitrarily functionally graded polar orthotropic rotating discs. Journal of the Brazilian Society of Mechanical Sciences and Engineering, 40(1), 1–21. https://doi.org/10.1007/s40430-018-1216-3

[5] Zhao, M. H., Dang, H. Y., Fan, C. Y., & Chen, Z. T. (2003). Analysis of an arbitrarily shaped interface cracks in a three dimensional isotropic thermoelastic bi-material. Part 1: Theoretical solution. International Journal of Solids and Structures, 40(8), 929–952. https://doi.org/10.1016/S0020-7683(02)00571-4

[6] Dai, T., Li, B., Tao, C., He, Z., & Huang, J. (2022). Thermo-mechanical analysis of a multilayer hollow cylindrical thermal protection structure with functionally graded ultrahigh-temperature ceramic to be heat resistant layer. Aerospace Science and Technology, 124, 107532. https://doi.org/10.1016/j.ast.2022.107532
[7] Iqbal, M. D., Birk, C., Ooi, E. T., Pramod, L. N., Natarajan, S., Gravenkamp, H., & Song, C. (2022). Thermoelastic fracture analysis of functionally graded materials using the scaled boundary finite element method. Engineering Fracture Mechanics, 264, 108305. https://doi.org/10.1016/j.engfracmech.2022.108305
[8] Riley, F. L. (2009). Silicon nitride and related materials. Journal of the American Ceramic Society, 83(2), 245–265. https://doi.org/10.1111/j.1551-2916.1999.tb20092.x
[9] Chen, L., & Wang, H. (2012). Advanced ceramic materials for aerospace applications. Journal of Aerospace Engineering, 25(3), 145–158. https://doi.org/10.1061/(ASCE)AS.1943-5525.0000135
[10] Zeng, P. (2015). Thermal shock behavior of ceramics: Testing and analysis. Ceramics International, 41(9), 10535–10542. https://doi.org/10.1016/j.ceramint.2015.04.024
[11] Timoshenko, S., & Goodier, J. N. (1970). Theory of elasticity. McGraw-Hill.
[12] AZoM. (2025). Sintered silicon nitride (Si_3N_4) – Properties. AZoM.com. Retrieved September 22, 2025, from https://www.azom.com/properties.aspx?ArticleID=260
[13] Precision Ceramics. (2025). Silicon nitride (Si_3N_4) ceramic: Properties & applications. Precision Ceramics UK. Retrieved September 22, 2025, from https://precision-ceramics.com/materials/silicon-nitride/
[14] Imetra, Inc. (2025). Silicon nitride material properties. Retrieved September 22, 2025, from https://www.imetra.com/silicon-nitride-material-properties/